Available online at www.sciencedirect.com
SCIENCE DIRECT®
Journal of Solid State Chemistry 179 (2006) 812–823
JOURNAL OF SOLID STATE CHEMISTRY
www.elsevier.com/locate/jssc

Mixed oxides obtained from Co and Mn containing layered double hydroxides: Preparation, characterization, and catalytic properties

František Kovanda[a,*], Tomáš Rojka[a], Jana Dobešová[a], Vladimír Machovič[b], Petr Bezdička[c], Lucie Obalová[d], Květa Jirátová[e], Tomáš Grygar[c]

[a]*Department of Solid State Chemistry, Institute of Chemical Technology, Technická 5, 166 28 Prague, Czech Republic*
[b]*Laboratory of Molecular Spectroscopy, Institute of Chemical Technology, Technická 5, 166 28 Prague, Czech Republic*
[c]*Institute of Inorganic Chemistry, Academy of Sciences of Czech Republic, 250 68 Řež, Czech Republic*
[d]*Technical University of Ostrava, 17. listopadu 15, 708 33 Ostrava, Czech Republic*
[e]*Institute of Chemical Process Fundamentals, Academy of Sciences of Czech Republic, Rozvojová 135, 165 02 Prague, Czech Republic*

Received 16 September 2005; received in revised form 29 November 2005; accepted 4 December 2005
Available online 5 January 2006

Abstract

Co–Mn–Al layered double hydroxides (LDHs) with various Co:Mn:Al molar ratios (4:2:0, 4:1.5:0.5, 4:1:1, 4:0.5:1.5, and 4:0:2) were prepared and characterized. Magnesium containing LDHs Co–Mg–Mn (2:2:2), Co–Mg–Mn–Al (2:2:1:1), and Co–Mg–Al (2:2:2) were also studied. Thermal decomposition of prepared LDHs and formation of related mixed oxides were studied using high-temperature X-ray powder diffraction and thermal analysis. The thermal decomposition of Mg-free LDHs starts by their partial dehydration accompanied by shrinkage of the lattice parameter c from ca. 0.76 to 0.66 nm. The dehydration temperature of the Co–Mn–Al LDHs decreases with increasing Mn content from 180 °C in Co–Al sample to 120 °C in sample with Co:Mn:Al molar ratio of 4:1.5:0.5. A subsequent step is a complete decomposition of the layered structure to nanocrystalline spinel, the complete dehydration, and finally decarbonation of the mixed oxide phase. Spinel-type oxides were the primary crystallization products. Mg-containing primary spinels had practically empty tetrahedral cationic sites. A dramatic increase of the spinel cell size upon heating and analysis by Raman spectroscopy revealed a segregation of Co-rich spinel in Co–Mn and Co–Mn–Al specimens. In calcination products obtained at 500 °C, the spinel mean coherence length was 5–10 nm, and the total content of the X-ray diffraction crystalline portion was 50–90%. These calcination products were tested as catalysts in the total oxidation of ethanol and decomposition of N_2O. The catalytic activity in ethanol combustion was enhanced by increasing (Co + Mn) content while an optimum content of reducible components was necessary for high activity in N_2O decomposition, where the highest conversions were found for calcined Co–Mn–Al sample with Co:Mn:Al molar ratio of 4:1:1.

Keywords: Layered double hydroxides; Hydrotalcite-like compounds; Thermal decomposition; Cobalt–manganese mixed oxides; VOC combustion; N_2O decomposition

1. Introduction

Mixed oxides containing transition metal cations are often used as heterogeneous catalysts of many chemical reactions. These oxides are usually prepared by thermal decomposition of various precursors, e.g. hydroxides, carbonates, nitrates, oxalates, etc. Mixed-oxide-based catalysts can easily be obtained by a controlled thermal decomposition of the layered double hydroxides (LDHs), which are also known as hydrotalcite-like compounds or anionic clays [1,2]. The chemical composition of LDHs may be represented by the general formula $[M^{II}_{1-x}M^{III}_{x}(OH)_2]^{x+}[A^{n-}_{x/n}\cdot yH_2O]^{x-}$ where M^{II} and M^{III} are divalent and trivalent metal cations, A^{n-} is an n-valent anion and x has usually values between 0.25 and 0.33. After heating at moderate temperatures, LDHs give finely dispersed mixed oxides of M^{II} and M^{III} metals with high surface area and good thermal stability that is usually required for heterogeneous catalysts. A great number of

*Corresponding author. Fax: +420 224311082.
E-mail address: Frantisek.Kovanda@vscht.cz (F. Kovanda).

0022-4596/$ - see front matter © 2005 Elsevier Inc. All rights reserved.
doi:10.1016/j.jssc.2005.12.004

studies on thermal decomposition of LDHs were performed with synthetic Mg–Al hydrotalcite [3–6]. Two characteristic processes accompanied by a considerable weight loss and an endothermic effect can be observed during hydrotalcite heating: the release of interlayer water at 150–200 °C accompanied by a collapse of the LDH basal spacing [7,8] and by the complete decomposition of the layered structure at 350–600 °C. The resulting structurally disordered oxide mixture crystallizes to new phases, a process with kinetics strongly depending on the metal ion constituents. Mg–Al hydrotalcite yields a periclase (MgO) phase above 400 °C and $MgAl_2O_4$ spinel above 900 °C. $M^{II}M_2^{III}O_4$ spinel-like phase and/or divalent metal single or mixed oxides $M^{II}O$ are usually detected in the powder X-ray diffraction (XRD) patterns of M^{II}–M^{III} LDHs calcined at high temperatures. The ill-organized mixed oxides obtained at lower temperatures display generally three broad diffraction maxima corresponding to the future strongest lines of the spinel- or periclase-like phase. Therefore, they are also called pre-spinel oxides and a topotactic transformation from the layered structure to this oxide phase may be considered [9].

Both cobalt and manganese cations can attain variable oxidation states and may be the effective components in mixed-oxide-based catalysts suitable for redox reactions. For example, Co-containing mixed oxides prepared from hydrotalcite-like precursors were tested in the catalytic decomposition of nitrous oxide [10,11] and in the selective catalytic reduction of NO with ammonia [12]. Co and Mn oxides have also been reported as catalysts used in the combustion of volatile organic compounds [13]. Thermal decomposition of Co-based LDHs results in the formation of homogeneous spinel-type oxides at relatively low temperature [14,15]. A diffuse pattern, exhibiting both tenorite and spinel phases, was obtained after calcination of ternary Cu–Co–Al hydrotalcites at 500 °C [16]. Preparation and properties of mixed oxides formed after calcination of Co–Fe LDHs are studied in [17]. In the products obtained at high calcination temperature of 1200 °C, $CoFe_2O_4$ spinel was the dominant phase; samples with higher Co/Fe molar ratio contained also different amounts of Co_3O_4 and CoO. During thermal treatment of Mg–Mn LDH, the hydrotalcite structure collapsed at 390 °C; only broad and weak diffraction peaks corresponding to both MgO and spinel phases were observed. At higher calcination temperatures, Mg_2MnO_4 spinel was detected [18].

In our recent papers [19–22], we have studied the crystallization of mixed oxides during calcination of LDH precursors containing Cu or Ni together with Mn cations in hydroxide layers. Heating of these compounds yielded dominant spinel-like oxides, but practically each system has some peculiarity given by specific properties of the constituents. In Cu-containing systems, early crystallization of CuO was found. A nanocrystalline periclase-like phase is primarily formed in Mg-rich systems [19]. The Ni-containing systems yield mixed oxide $(Ni,Mg,Mn^{IV})O$ with disordered murdochite structure, Ni_6MnO_8 (murdochite) and $NiMnO_3$ (ilmenite) as primary crystalline phases, and Mn^{IV} rich amorphous intermediate [20,22]. If the oxides should be used as catalysts, the product obtained at moderate calcination temperatures resulting in the high surface area and a rather poor crystallinity of the oxide mixture is required, and therefore the phase composition cannot be simply estimated from the thermodynamics and phase diagrams. The structural development of any new system must hence be experimentally established.

In the present study, the formation of mixed oxides during thermal treatment of layered double hydroxides containing Co and Mn cations in combination with Mg and/or Al ones is studied using various analytical methods. One of these oxides, containing Co, Mn, and Al, has been recently found to be efficient catalyst of N_2O decomposition [21]. Therefore, the catalytic properties of studied LDHs calcined at 500 °C were tested, both in decomposition of nitrous oxide and total oxidation of ethanol to relate their catalytic activity and phase composition as a mean to better understanding the structure–property relationship.

2. Experimental

2.1. Preparation of samples

Eight LDH-type precursors containing different amounts of Co and Mn cations were prepared by coprecipitation. The samples were denoted by acronyms with elemental composition and the molar ratios of the constituents. For example, Co4MnAl sample contained Co, Mn, and Al in molar ratio of 4:1:1. The following samples were obtained: Co4Al2, Co4Mn0.5Al1.5, Co4MnAl, Co4Mn1.5Al0.5, Co4Mn2, Co2Mg2Al2, Co2Mg2MnAl, and Co2Mg2Mn2. An aqueous solution (450 ml) of appropriate nitrates, i.e. $Co(NO_3)_2 \cdot 6H_2O$, $Mg(NO_3)_2 \cdot 6H_2O$, $Mn(NO_3)_2 \cdot 4H_2O$, and $Al(NO_3)_3 \cdot 9H_2O$, with $(Co+Mg)/(Mn+Al)$ molar ratio equal to 2 and total metal ion concentration of $1.0\,mol\,l^{-1}$ was added with flow rate of $7.5\,ml\,min^{-1}$ into 100 ml mixed flow reactor. The flow rate of simultaneously added alkaline solution of 0.5 M Na_2CO_3 and 3 M NaOH was controlled to maintain reaction $pH = 10.0 \pm 0.1$. The coprecipitation was carried out under vigorous stirring at 25 °C. The resulting suspension was drained to thermostated tank, where it was stirred 2 h at 25 °C. The product was filtered off, washed several times with distilled water, and dried overnight at 60 °C in air. The dried products were heated 2 h at chosen temperatures in the range 100–1100 °C in air and then cooled to the room temperature. The heated samples were used for the XRD, Raman, and surface area measurements.

The mixed oxide catalysts were prepared by following way: The washed and dried LDH precursors were formed into extrudates and then calcined at 500 °C for 4 h in air. The calcined extrudates were crushed and sieved to obtain the fraction of particle size 0.160–0.315 mm, which was used in TPR and catalytic measurements.

Reference spinel oxide Co_3O_4 was prepared by calcination of freshly precipitated basic Co-carbonate at 300 °C for 10 h. Mixed oxides $(Co_{0.9}Mn_{0.1})_3O_4$ and $(Co_{0.7}Mn_{0.3})_3O_4$ were obtained by evaporation of aqueous solution of the corresponding metal nitrates with citric acid, and calcination of the resulting dry foam at 900 °C for 10 h. The products were, according to XRD, single-phase spinels.

2.2. Techniques

Thermal analyses, including thermogravimetry (TG), differential thermal analysis (DTA) and evolved gas analysis (EGA), were carried out using a Netzsch STA 409 instrument equipped by the quadrupole mass spectrometer QMS 403/4 (Balzers). The heating rate of 5.6 °C min^{-1}, air with flow rate of 75 ml min^{-1} and 50 mg of sample were used. Gaseous products were continually monitored for chosen mass numbers m/z (18-H_2O^+ and 44-CO_2^+).

Powder XRD patterns were recorded using a Seifert XRD 3000P instrument with Co$K\alpha$ radiation ($\lambda = 0.179$ nm, graphite monochromator, goniometer with the Bragg–Brentano geometry) in 2θ range 12–75°, step size 0.05°. Rayflex and PowderCell 2.4 were used for phase identification as described in our previous reports [19,20]. For refinement of lattice parameters and estimation of the mean coherence length (approximately equal to crystallite size), DiffracPlus Topas, release 2000 (Bruker AXS, Germany) was used. The structural models were taken from the Inorganic Crystal Structure Database ICSD/Retrieve 2.01 (FIZ Karlsruhe, Germany).

High-temperature powder XRD (HT XRD) was performed in Anton Paar HTK16 high-temperature chamber with PANalytical X'Pert PRO diffractometer (Co$K\alpha$ radiation, X'Celerator multichannel detector). The detector enabled us the acquisition of detailed XRD patterns within several minutes that is useful in approaching the course of thermal decomposition monitored by TG/DTA/EGA. To study the precursor decomposition and oxide phases crystallization, we scanned in 2θ range 4–80° (Co$K\alpha$) with an effective heating rate of 0.85 °C min^{-1} between 25 and 400 °C (the step of 25 °C) and then the heating rate was raised to 3.3 °C min^{-1} between 400 and 900 °C (the step of 100 °C). To obtain a more detailed insight into the LDHs decomposition, we used a faster heating program with scanning in 2θ range 11–18° (Co$K\alpha$) with an effective heating rate of 5.6 °C min^{-1} between 25 and 350 °C (the step of 10 °C). The thermal evolution of the selected diffractograms was processed using OriginPro 7.5 with Peak Fitting Module (Origin Lab, USA); the line position, width, and area were estimated by its fitting to PseudoVoigt1 peak function. HT XRD measurements were used to identify LDHs decomposition temperatures and estimate the thermal dependence of the relative amount of crystalline spinel in the calcined samples.

Raman spectra were collected using the LabRam HR system (Jobin Yvon). The 532 nm line of 50 mW laser was used for excitation. The scattered light was analyzed by spectrograph with holographic grating (600 gr/mm), slit width 150 μm and opened confocal hole (1000 μm). The system adjustment was regularly checked using a silicon sample and by measurement in the zero-order position of the grating. The time of acquisition of a particular spectral window was optimized for individual sample measurements (ca. 200–400 s). The spectra were fitted using the Peak Fitting Module in OriginPro 7.5.

The chemical composition of the samples was determined by AAS after sample dissolution in hydrochloric acid. The average error of the determination was about 3% rel. The metal ion redox state was determined by iodometry or by permanganometeric back-titration after sample dissolution in an acidified solution of $(NH_4)_2Fe(SO_4)_2$ (Mohr salt) as described in our previous reports [19,20,22]. Iodometry, i.e. dissolution in excess KI in cold diluted HCl, is more convenient but it was only applicable in samples obtained at lower calcination temperatures (< 500 °C). The less reactive samples obtained at higher temperatures had to be dissolved in diluted H_2SO_4 and H_3PO_4 under heating in nitrogen atmosphere with stirring and ultrasonication. The methods yielded the same results within a common error of estimation (3–5% rel.). In both these analyses, total-oxidizing equivalents (in mmol/g) corresponding to cations Co^{3+}, Mn^{3+}, and Mn^{4+} were determined. The results expressed as an average (Co + Mn) valence were obtained by dividing total oxidizing equivalents to total (Co + Mn) concentration (in mmol/g) and adding the results to number 2 ("non-oxidizing" valence of Co and Mn); the valence of Mg and Al was assumed being constant 2+ and 3+, respectively.

Surface area measurements were carried out on a PulseChemisorb 2700 instrument (Micromeritics) by dynamic chromatographic method. All samples were predried in air at 150 °C for 3 h, except dried precursors and samples heated at 100 °C, which were pre-dried at 60 and 100 °C, respectively. Surface area of the samples was evaluated following the three-point BET method by nitrogen adsorption at 77 K. The N_2 concentrations of 5, 15, and 30 vol% in the nitrogen–helium mixture were used.

Temperature-programmed reduction (TPR) measurements were carried out with 50 mg sample weight in a hydrogen–nitrogen mixture (10 mol% H_2) with flow rate of 15 ml min^{-1}. The temperature was linearly raised at the rate of 20 °C min^{-1} up to 850 °C. After freezing of rising water at −76 °C, a composition of gases was analyzed by thermal-conductivity detector.

The catalytic activity in total oxidation of ethanol was determined in an integral catalytic reactor of 7 mm internal diameter with 0.75 g of catalyst, ethanol concentration in the air of 1.0 g m^{-3} and the flow rate of the reaction mixture through the catalyst of 2.5 l h^{-1}. The oxidation of ethanol was carried out under unsteady-state reaction temperature with heating rate 3.5 °C min^{-1} within the limits 50–400 °C. The composition of the gas mixture in the reactor inlet and outlet was determined using gas

chromatograph Hewlett-Packard 6890 equipped by FID detector. The T_{50} temperature, at which 50% conversion of ethanol was observed, was chosen as a measure of the catalytic activity.

The N_2O decomposition reaction was performed in fixed bed reactor of 5 mm internal diameter in temperature range 330–450 °C with total flow rate of 50–100 ml min^{-1} NTP (273 K, 101.325 kPa), 0.1–0.3 g of catalyst and 1000 ppm N_2O balanced by helium. Before each run, the catalyst was pre-treated by heating in the helium flow (50 ml min^{-1}, heating rate 10 °C min^{-1}) up to 450 °C and maintaining the temperature for 1 h. Then the catalyst was cooled to reaction temperature and the steady state of N_2O at the reactor output was measured. The gas chromatograph Hewlett Packard 5890, series II GC equipped by TCD detector was used to determine N_2O concentration in the reactor inlet and outlet.

3. Results and discussion

3.1. Characterization of prepared precursors

Chemical analyses of the dried precursors are summarized in Table 1. The molar ratios of cations in solids corresponded approximately to those in the nitrate solutions used for coprecipitation. A low amount of remaining sodium cations was also found in the washed and dried samples.

In the powder XRD patterns of Co4Al2, Co4Mn0.5Al1.5, Co4MnAl, Co2Mg2Al2 and Co2Mg2MnAl dried precursors, only a well-crystallized hydrotalcite-like phase was detected (Fig. 1). A hydrotalcite-like phase was predominant also in the powder XRD pattern of the Co2Mg2Mn2 precursor but it exhibited a lower crystallinity in comparison with the other samples and contained a slight amount of MnOOH (feitknechtite) as an admixture. In the XRD patterns of $Co_4Mn_{1.5}Al_{0.5}$ and Co_4Mn_2 precursors, an unidentified phase with d~0.665 nm was found. This unidentified phase was a major component in the Co4Mn2 sample, while in the Co4Mn1.5Al0.5 sample it was found only as an admixture of LDH. The absence of hydrotalcite-like phase in XRD pattern of Co4Mn2 sample was in line with a very low content of carbonate and high mean (Co + Mn) valence (Table 1).

The LDH lattice parameter a increases with increasing Mn/Al ratio in the samples that proves Mn incorporation into the hydroxide layers of hydrotalcite-type lattice (Table 2).

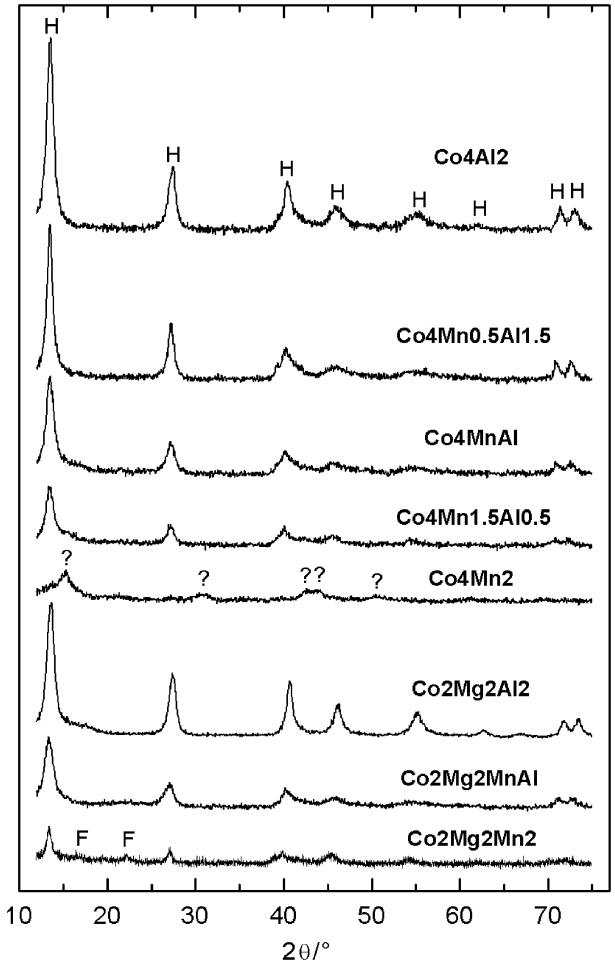

Fig. 1. XRD patterns of prepared LDH precursors dried at 60 °C. Phase abbreviations: H—hydrotalcite, F—feitknechtite (MnOOH), ?—unidentified phase.

Table 1
Chemical composition and mean (Co + Mn) valence of prepared precursors dried at 60 °C

Sample	Co (wt%)	Mg (wt%)	Mn (wt%)	Al (wt%)	CO_3^{2-} (wt%)	Na (wt%)	Co:Mg:Mn:Al molar ratio	(Co + Mn) valence
Co4Al2	35.8	—	—	8.57	9.93	0.022	4.00:0:0:2.09	n.d
Co4Mn0.5Al1.5	35.7	—	4.20	6.20	8.72	0.044	4.00:0:0.50:1.52	2.21
Co4MnAl	35.2	—	8.60	4.23	7.24	0.022	4.00:0:1.05:1.05	2.34
Co4Mn1.5Al0.5	37.3	—	12.8	2.20	6.42	0.012	4.00:0:1.47:0.52	2.60
Co4Mn2	43.0	—	20.6	—	0.92	0.193	4.00:0:2.06:0	2.88
Co2Mg2Al2	20.4	8.44	—	9.35	11.5	0.187	2.00:2.01:0:2.00	n.d.
Co2Mg2MnAl	20.2	7.84	10.0	4.76	8.72	0.067	2.00:1.88:1.06:1.03	2.48
Co2Mg2Mn2	21.0	6.64	20.8	—	13.0	0.015	2.00:1.53:2.13:0	2.58

n.d.—not determined.

3.2. Thermal decomposition of the LDH precursors

The course of the LDHs decomposition was monitored by conventional thermal analysis (TG/DTA/EGA) and additionally by high-temperature X-ray diffraction (HT XRD). HT XRD of LDHs was first discussed by Kanezaki [7], the mechanism of the LDH collapse was explained by Stanimirova et al. [8] and the method was used to study the LDH conversion to oxides by Pérez-Ramírez et al. [14]. HT XRD analysis of Co- and Mn-containing LDHs has not been described in the literature yet. In agreement with the literature data on Mg–Al LDHs [7,8], Co-containing LDHs studied in this work (the principal basal spacing of d~0.76 nm) were first converted to a collapsed LDH with basal spacing of d~0.66 nm (Table 3). The collapsed phase retaining the layered structure of the precursor was denoted as Phase II [7] or metahydrotalcite B [8] and was denoted as collapsed LDH in this work.

Thermoanalytical curves (TG/DTA) of the selected precursors together with analysis of evolved gases (H_2O and CO_2) are shown in Fig. 2 and an example of HT XRD scans is shown in Fig. 3. The characteristic temperatures obtained by TG/DTA/EGA and HT XRD scans are listed in Table 3. Samples Co4Al2, Co4MnAl and Co2Mg2MnAl exhibited two major endothermic effects typical for hydrotalcite-like compounds, the first being associated with a release of interlayer water and the second with a H_2O and CO_2 release associated with the complete dehydroxylation of hydroxide layers, decomposition of interlayer carbonate anions and destruction of layered LDH structure. The first, more pronounced endothermic minimum was found at 230 °C in Co4Al2 and at 180 °C in Co4MnAl and Co2Mg2MnAl samples. The temperatures of the collapse of the LDH structures according to HT XRD were, however, significantly lower than the thermal effects found in DTA curves and maximum decay rates by TG/EGA. Comparing the HT XRD and thermal analysis results, it can be considered that already a slight dehydration of the LDH precursors leads to a collapse of the original LDH structure accompanied by the shrinkage of LDH basal spacing from about 0.76 to 0.66 nm; a marked water evolution is detected by thermal analysis at higher temperatures. The evolution of H_2O was complete simultaneously (Co4Al2 sample) or soon after the total decay of the collapsed layered structure. Surprisingly, the major part of CO_2 was evolved after that dehydration step, and at temperature higher than temperature corresponding to the complete decay of collapsed LDH structure. In other words, CO_2 was mostly evolved from crystallographically disordered oxide mixture.

The proposed reaction model of structural changes preceding the evolution of the gaseous products is supported by the course of the decomposition of Co2Mg2Mn2 and Co2Mg2MnAl samples. HT XRD revealed that the Co2Mg2Mn2 LDH was completely decayed at about 120 °C, with a corresponding collapsed LDH form practically absent in the diffraction pattern. The primary product of Co2Mg2Mn2 decay was almost XRD amorphous. However, the endothermic effect accompanied by H_2O evolution was found at DTA curve at 160 °C; the second endothermic effect connected with evolution of remaining H_2O and the partial sample decarbonation was found at 280 °C. The remaining CO_2 was evolved at much higher temperature of about 550 °C. Such a high-temperature release of residual carbonate has been also observed during heating of LDHs containing Cu, Mg, and Mn [20], Ni, Cu, and Al [23] and Cu and Al [24]. It is probably related to a very strong chemisorption of CO_2 on the oxide mixture after LDHs decay, because no crystalline carbonate species was found by XRD in any of

Table 2
Lattice parameters of the prepared LDHs

Sample	a (10^{-10} m)	c (10^{-10} m)
Co4Al2	3.066	22.63
Co4Mn0.5Al1.5	3.077	22.76
Co4MnAl	3.084	22.81
Co4Mn1.5Al0.5	3.097	22.86
Co2Mg2Al2	3.055	22.67
Co2Mg2MnAl	3.076	22.91
Co2Mg2Mn2	3.093	22.81

Table 3
Thermal decomposition characteristics of LDHs obtained by DTG (the temperature of DTG maxima), EGA (temperatures of maximum H_2O and CO_2 evolution), and HT XRD (temperatures of the half-integral intensity of the species)

Sample	T of Δm maxima (°C) (DTG)	$-H_2O$ (°C) (EGA)	$-(H_2O)$, $-CO_2$ (°C) (EGA)	LDH collapse (°C) (HT XRD)	Basal spacing of collapsed LDH (10^{-10} m) (HT XRD)	LDH decay (°C) (HT XRD)
Co4Al2	226; 255	235	257	180	6.65 (220 °C)	260
Co4Mn0.5Al1.5	186; 230	194	236	150	6.56 (175 °C)	210
Co4MnAl	169; 214	171	219	130	6.67 (150 °C)	200
Co4Mn1.5Al0.5	150; 197	158	200	120	6.63 (150 °C)	170
Co2Mg2Al2	209; 320	220	328	190	6.67 (210 °C)	290
Co2Mg2MnAl	160; 300	170	308	140	6.58 (175 °C)	240
Co2Mg2Mn2	139; 275	151	269	110	not formed	not formed

DTG—derived thermogravimetric results.

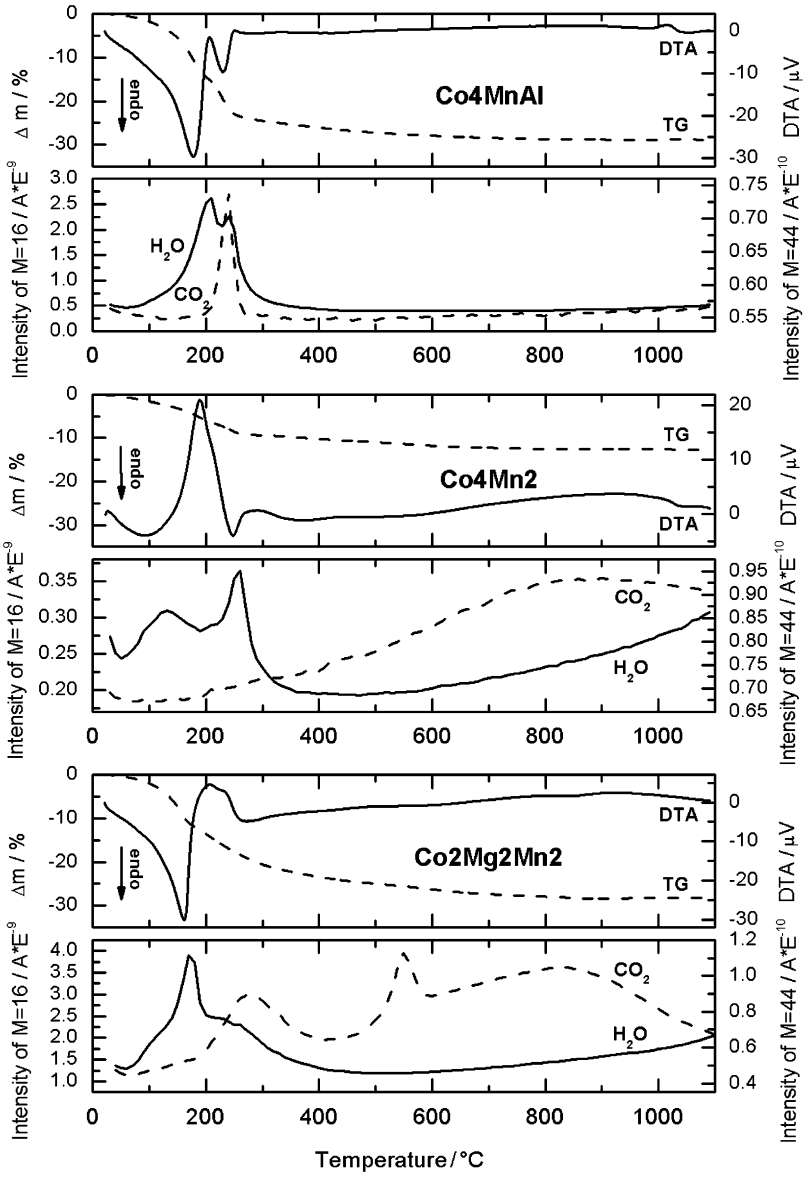

Fig. 2. Results of thermal analysis (TG/DTA/EGA) of Co4MnAl, Co4Mn2 and Co2Mg2Mn2 precursors.

the mentioned cases. The decarbonation maximum of Co2Mg2MnAl sample was found at temperatures substantially exceeding the thermal stability of the collapsed LDH. The decay of the two Mg-containing specimens hence demonstrates that some of the decomposition reactions are due to conversions of crystallographically disordered (amorphous) species, not to collapsed LDHs. The thermal stability of the collapsed LDHs increased with increasing Al/Mn ratio. Similarly, Kanezaki [7] found an increased thermal stability of Mg–Al LDH with higher Al/Mg ratio.

Thermal behavior of Co4Mn2 sample was quite different. As followed from chemical and XRD analyses, the Co4Mn2 precursor was not a LDH. The unassigned diffraction line at d~0.665 nm disappeared, according to HT XRD, between 200 and 225 °C. During heating of the Co4Mn2 sample, two major endothermic effects with minima at approximately 100 and 245 °C were observed and the course of DTA curve was similar to that measured with LDH-type samples. However, both these minima were associated with evolution of water, which can be explained by dehydroxylation of unidentified, probably hydroxide- and/or oxohydroxide-type phases. The TG measurements showed that the release of water was accompanied by total weight loss of about 10%, which is much lower than weight loss observed for the other studied LDH precursors (about 25–30%). Analysis of evolved gases did not show any evolution of CO_2, which is in agreement with very low content of carbonate determined by chemical analysis.

3.3. The early stages of crystallization of oxide phases

The total thermal decomposition of LDHs above 200–260 °C (Table 3) proceeded in two ways depending on a contingent presence of Mg. In all Mg-free samples

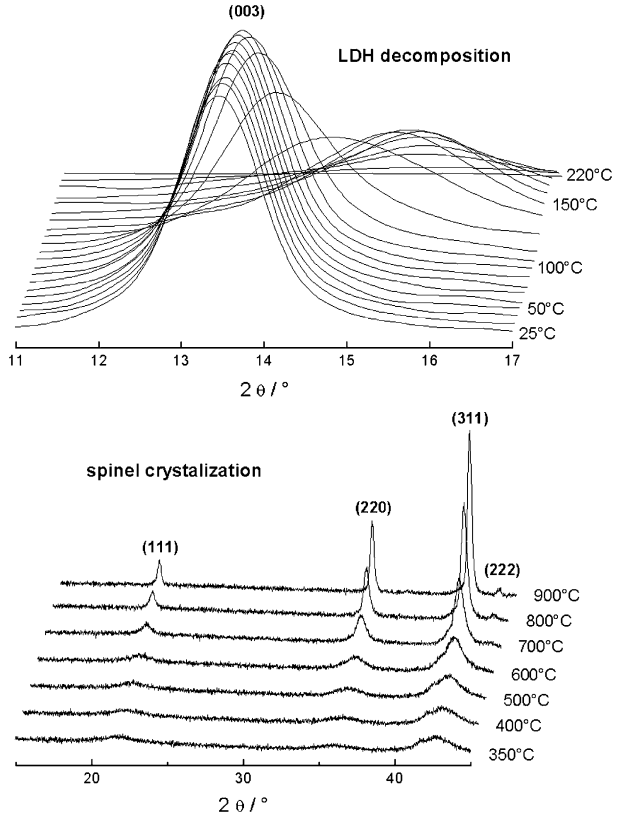

Fig. 3. HT XRD pattern of Co4MnAl sample.

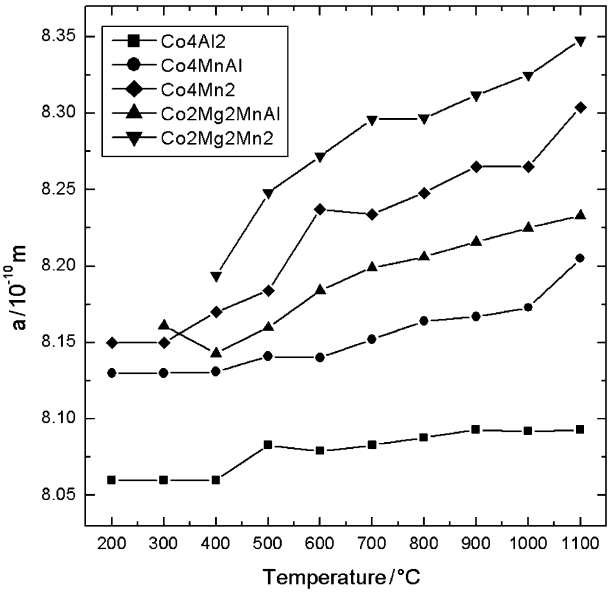

Fig. 4. Temperature dependence of the spinel lattice parameter *a* in the selected calcined samples (ambient XRD measurements).

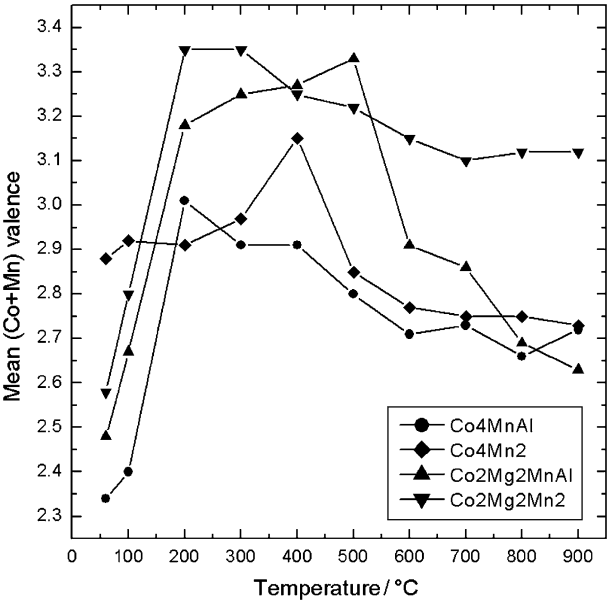

Fig. 5. Mean (Co + Mn) valence in the selected precursors and related calcined samples in dependence on calcination temperature.

studied, nanocrystalline spinels were formed at relatively low temperatures, practically immediately after the total decay of the precursors. The spinel (220) and (311) diffraction lines arose immediately after the decomposition of the collapsed LDH, however, in some cases, especially in Mg-containing Co2Mg2Mn2 and Co2Mg2MnAl samples, the ratio between their integral intensities was temperature-dependent. Particularly the ratio of areas of (220) line to (311) line increased with increasing temperature. The usual spinel-like diffraction pattern was gradually developed at temperatures above 500 °C. The ratio between spinel diffraction lines (111) and (220) is a measure of the occupancy of the tetrahedral cationic sites: when those sites are empty, the (220) line is absent. Hence, the intermediate spinel phase of Mg-containing samples calcined at 300–400 °C had cations mainly in octahedral positions, i.e. in the same surrounding as in the precursor.

Similarly as in previous cases of LDH-derived oxide mixtures containing transition metal cations [19,22], the spinel lattice parameter *a* increased as the mean valence of the metal ions decreased at higher calcination temperatures (Figs. 4 and 5). The mean (Co + Mn) valence reached its maximum at 200–500 °C, i.e. immediately after the decay of the layered structure of the precursors. The considerable increase of mean (Co + Mn) valence observed at lower calcination temperatures can be explained by a partial Co^{II} to Co^{III} and likely Mn^{III} to Mn^{IV} oxidation as well, which takes place during the LDH decomposition in air followed by spinel phase formation. With further heating, the gradual crystallization of spinels takes place and the mean (Co + Mn) valence continuously decreases due to an ordering of the spinel structure. The increase of the spinel lattice parameter is caused partly due to larger ionic radii of Co and Mn at lower valence states. A particular feature of the oxide mixtures containing Co and Mn is the magnitude of the increase of the unit cell size of spinel on heating. That is much larger than in the corresponding systems containing Cu and Mn [19] or Ni and Mn [22] although the decrease of the mean valence of the metal ions

is comparable in all these systems. The growth of the unit cell size a is largest during calcination of Co4Mn2 sample, where the primary spinel phase observed at 200 °C has $a \sim 0.815$ nm, that is close to Co_3O_4 ($a = 0.8084$ nm, PDF-2 card No. 42-1467). A spinel remained the only phase up to 900 °C, but its a value grew to 0.8265 nm that is very close to stoichiometric Co_2MnO_4 ($a = 0.8269$ nm, PDF card No. 23-1237). This large increase of a value is accompanied by only a moderate change in the mean (Co + Mn) valence. The actual occupation of the spinel lattice by individual elemental constituents cannot be obtained by XRD data processing, because their X-ray scattering power is very similar.

In aim to prove the elemental segregation in the oxide mixture, we used Raman spectroscopy, which can sometimes distinguish between crystallographically similar phases with a different elemental composition. For example, non-stoichiometric spinel oxides have generally very variable coordination surrounding in the nearest and next-nearest metal-ion neighbors, while local symmetry in oxides with a fixed stoichiometry is much higher. This difference can affect the width of the bands in vibrational–rotational spectra. We used this approach in identification of stoichiometric oxide $(Ni,Mg)_6MnO_8$ beside the non-stoichiometric spinel oxides by Raman spectroscopy [20].

The Raman bands of Co_3O_4 are sharper than that of non-stoichiometric Co,Mn-containing spinels, and with Mn incorporation into the lattice, the bands of Co_3O_4 are shifted, broadened, and some of them coalesce. For example, a pair of bands at 469 and 511 cm^{-1} with FWHM of 14 cm^{-1} in Co_3O_4 is coalesced to a single band at 488 cm^{-1} with FWHM of 52 cm^{-1} in $(Co_{0.7}Mn_{0.3})_3O_4$. The change of the Raman spectra of Co4Mn2 calcined samples and reference Co,Mn-spinels are compared in Fig. 6. The results hence proved that the primary spinel formed in Co4Mn2 calcination products is Co-enriched, and the Mn incorporation into the spinel lattice proceeds during its further recrystallization. The behavior of Co4MnAl system was similar, the sharp Raman bands resembling Co_3O_4 developed in calcined samples obtained between 400 and 600 °C and changed to broad bands of non-stoichiometric spinel at 700 °C.

The Raman spectra of the calcined Co4Al2 samples were quite different. Between 400 and 800 °C, the band position was changed by about few cm^{-1}, and the bandwidth decreased monotonously. Such a slight shift and band sharpening is typical for mere growth of the particles of transition metal oxides [25].

3.4. Thermal evolution of spinels

The calcined samples obtained at 500 °C were successfully tested as catalysts of N_2O decomposition [21]. At this temperature, the samples contained nanocrystalline spinel-like phases according to XRD. Their thermal crystallization proceeded in two ways: by the continuous conversion of the disordered material to X-ray diffracting

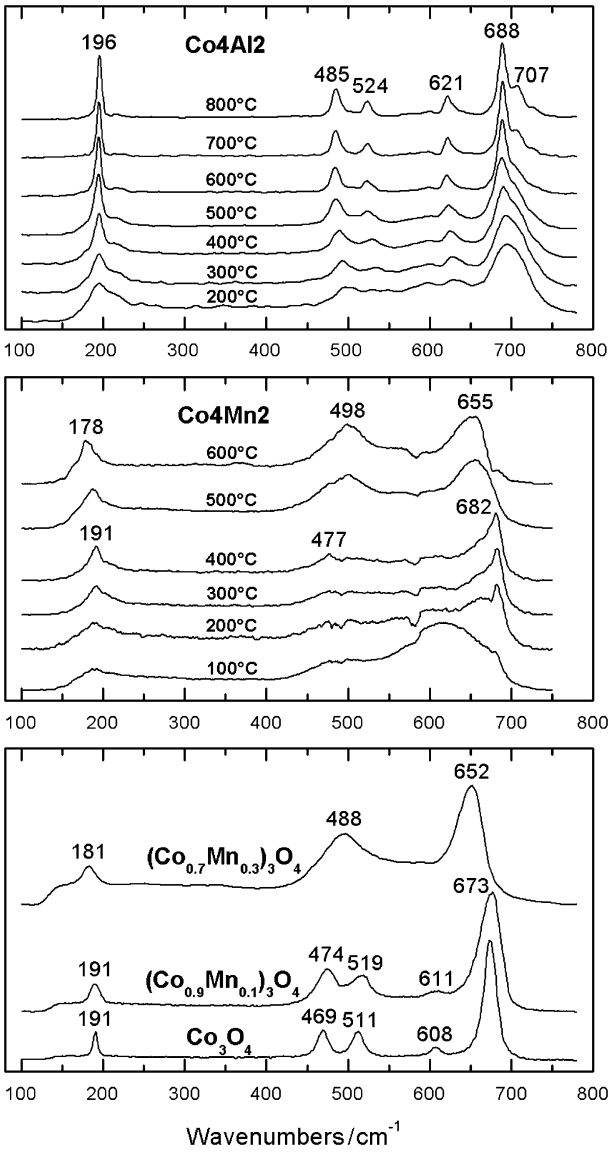

Fig. 6. Raman spectra of Co4Al2 and Co4Mn2 calcined samples in dependence on calcination temperature compared to Raman spectra of reference spinels.

oxides expressed as an increase of the integral intensities of the spinel diffraction lines (Fig. 7) and also by the growth of the spinel mean coherence length (Fig. 8). The gradual crystallization of spinels and contingent particle sintering at higher temperatures caused a significant decrease in the surface area with increasing calcination temperature (Fig. 9). The integral intensities of the spinel (311) diffraction line increased until reaching a stable maximum value at 800 (Co4Mn2 sample) or 900 °C (all other systems). We assumed that the maximum value of the integral intensity obtained at those temperatures corresponded to a completely XRD-ordered bulk of the calcined sample, and we estimated the content of XRD amorphous components at 500 °C as the relative ratio of the integral intensity of sample calcined at 500 °C to that maximum value. The most relevant XRD-derived parameters are

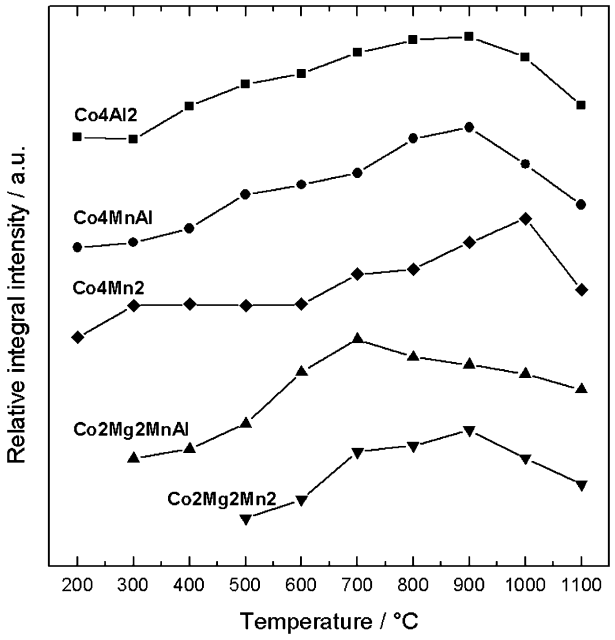

Fig. 7. Temperature dependence of the integral intensity of the spinel (511) diffraction line in the selected calcined samples (ambient XRD measurements).

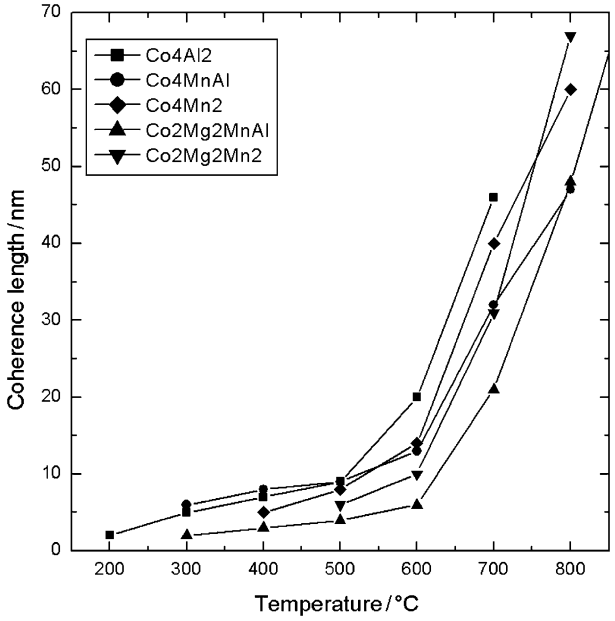

Fig. 8. Temperature dependence of the mean coherence length of the spinel in the selected calcined samples (calculated from spinel (511) diffraction line, ambient XRD measurements).

summarized in Table 4. The decrease of the integral intensity of the spinel diffraction lines at high temperatures above 900 °C can be explained by the phase transformation of calcination products when oxides CoO or (Co,Mg)O are formed to the detriment of spinels. These Co^{II}-containing cubic oxides were found together with spinels in the XRD patterns of samples calcined at high temperatures.

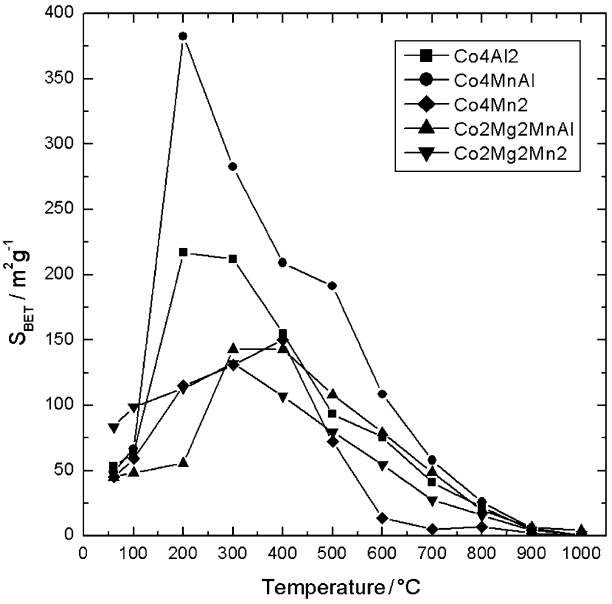

Fig. 9. Surface area of selected samples in dependence on calcination temperature.

Table 4
The characteristics of the calcined samples obtained at 500 °C

Sample	Crystalline fraction (%)[a]	Spinel lattice parameter a (10^{-10} m)[b]	Mean spinel coherence length (nm)[b]	Mean (Co + Mn) valence[c]
Co4Al2	89	8.083	9	n.d.
Co4Mn0.5Al1.5	85	8.101	10	n.d.
Co4MnAl	76	8.141	9	2.80
Co4Mn1.5Al0.5	70	8.130	10	2.84
Co4Mn2	63	8.184	8	2.85
Co2Mg2Al2	54	8.100	4	n.d.
Co2Mg2MnAl	46	8.160	4	3.33
Co2Mg2Mn2	74	8.248	6	3.22

n.d.—not determined.
[a]Integral intensity of spinel diffraction line (311) at 500 °C related to that at 900 °C, HT XRD.
[b]Evaulated from ambient XRD measurement.
[c]Evaluated from chemical analysis.

3.5. TPR results

TPR patterns of catalysts prepared by calcination of formed LDH precursors at 500 °C are demonstrated in Fig. 10. Two main temperature regions can be distinguished during reduction of Co–Mn and Co–Mn–Al samples. The first one (200–400 °C) was ascribed to reduction of Co components and the second one (400–750 °C) represented mainly reduction of Mn components. The low-temperature part consists of two reduction peaks associated with Co^{III} to Co^{II} reduction followed by reduction of Co^{II} to Co^0. The two-step reduction of Co_3O_4 was reported by Sexton et al. [26] and by Linn and Chen [27] but Arnoldy and Moulijn [28] observed the reduction of Co_3O_4 around 330 °C almost without distinguishing the

corresponding reduction peaks. Reduction of Mn oxides is more complex and can proceed via different reduction stages. Ferrandon et al. [29] reported the peaks with maxima at 328 and 424 °C during reduction of free MnO_x. Kapteijn et al. [30] observed analogous two peaks during reduction of β-MnO_2. The first one around 250 °C was ascribed to reduction of MnO_2 or Mn_2O_3 to Mn_3O_4, the second one at 360–440 °C to reduction of Mn_3O_4 to MnO.

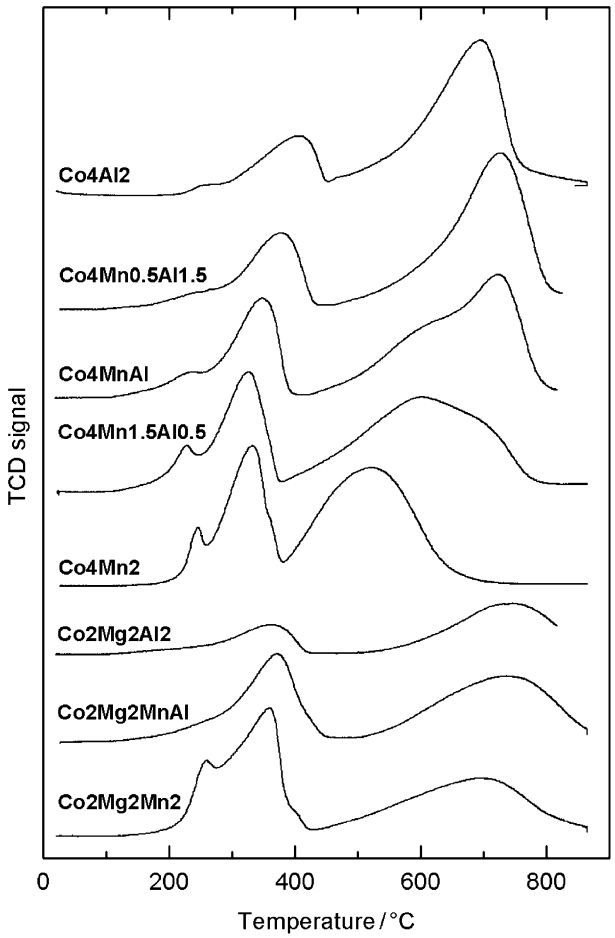

Fig. 10. Temperature-programmed reduction patterns of catalysts prepared by calcination of formed LDH precursors at 500 °C.

The incorporation of Al into the Co–Mn system caused only a slight change in the first reduction peak position but the second peak was shifted to higher temperatures indicating worse reducibility of the arising components of the catalysts. These results are in agreement with observations of Arnoldy and Moulijn [28] that Al^{3+} cations influence strongly the reducibility of cobalt cations and cause an increase in reduction temperature. This effect was explained by polarization of Co–O bonds by Al^{3+} ions. Temperature-programmed reduction of calcined Co–Al hydrotalcite was previously reported by Ribet et al. [31]. Occurrence of two distinct reducible cobalt species around 350 and 730 °C was assigned to the reduction of Co_3O_4 and spinel-like phase, respectively. Analogous reduction peaks were observed also in TPR patterns of calcined Co–Mg–Al hydrotalcite. The addition of magnesium to the Co_3O_4 did not change the course of reduction of Co^{III} to Co^{II} below 300 °C but it influenced the reduction of Co^{II} to Co^0. This effect was explained by reaction between CoO and MgO resulting in formation of CoO–MgO solid solution [31]. Cobalt in the CoO–MgO solid solution is reduced completely at much higher temperature (500–700 °C) in comparison with CoO, which is reduced at about 400 °C.

TPR data of studied catalysts are summarized in Table 5. The total amounts of hydrogen consumed during reduction in temperature range 20–800 °C corresponded with the content of reducible components (Co and Mn) in the catalysts. However, catalytic components reducible at temperatures higher than used reaction temperatures cannot likely contribute to the catalytic reaction. For that reason, the reducibility in the reaction temperature region used for N_2O decomposition was determined as the amount of hydrogen consumed in the range 350–450 °C.

3.6. Catalytic activity

The samples calcined at 500 °C were tested as catalysts in total oxidation of ethanol and decomposition of N_2O

Table 5
Surface area, TPR results, temperature T_{50} of ethanol combustion and rate constants of N_2O decomposition measured for catalysts prepared by calcination of formed LDH precursors at 500 °C

Catalyst	S_{BET} ($m^2\,g^{-1}$)	TPR: total H_2 consumption (20–800 °C) (mmol $H_2\,g^{-1}$)	TPR: H_2 consumption (350–450 °C) (mmol $H_2\,g^{-1}$)	T_{50}[a] (total oxidation of ethanol) (°C)	Rate constant[b] $k \times 10^{11}$ (mol $N_2O\,s^{-1}\,m^{-2}\,Pa^{-1}$)
Co4Al2	84.0	9.55	0.66	221	2.20
Co4Mn0.5Al1.5	103.2	10.70	1.56	175	6.60
Co4MnAl	92.7	11.26	0.96	169	15.6
Co4Mn1.5Al0.5	89.9	11.92	0.84	154	10.8
Co4Mn2	43.6	11.58	1.81	165	4.30
Co2Mg2Al2	106.3	6.69	0.80	229	2.18
Co2Mg2MnAl	91.7	7.47	1.77	232	1.89
Co2Mg2Mn2	57.3	9.75	1.57	172	2.64

[a]Temperature at which 50% conversion was achieved.
[b]Rate constant determined from the first-order kinetic expression (N_2O conversion <30%) at 420 °C.

(Figs. 11 and 12). The main results of catalytic tests are summarized in Table 5. The temperature T_{50}, at which 50% conversion was achieved, was chosen as a measure of catalytic activity of the prepared mixed oxides in ethanol combustion. The results showed statistically significant correlations between T_{50} values and (i) surface area of catalysts (direct proportionality), (ii) molar ratio of chemical constituents (Mg + Al)/(Co + Mn) (indirect proportionality), and (iii) total hydrogen consumption in TPR measurements (indirect proportionality). Hence, the most active catalysts are those with high (Co + Mn) content, with high hydrogen consumption in TPR and oxidation activity both related to the content of the redox active metals. The large surface area of the calcined samples is not crucial, as follows from the low T_{50} value measured for Co4Mn2 sample, which exhibited the low surface area but the high activity in ethanol total oxidation. The catalysts having higher surface area may also include micropores accessible for nitrogen but not accessible for the reactant. The part of surface area corresponding to micropores then cannot contribute to the catalytic reaction.

The temperature dependences of N_2O conversion are demonstrated in Fig. 12. The kinetic data of hydrotalcite-based catalysts can be fitted with the first-order rate law corresponding to no inhibition by oxygen [10]. Therefore, the rate constant k (mol $N_2O\,s^{-1}\,m^{-2}\,Pa^{-1}$) was evaluated according to the first-order expression (Table 5). It can be seen from Fig. 12 and Table 5 that the Co4MnAl catalyst was the most active. Although the surface area of catalyst is usually the critical parameter affecting its activity, a variation in specific surface area showed to have only a little effect. The obtained results indicate that an optimum amount of components reducible in the temperature region

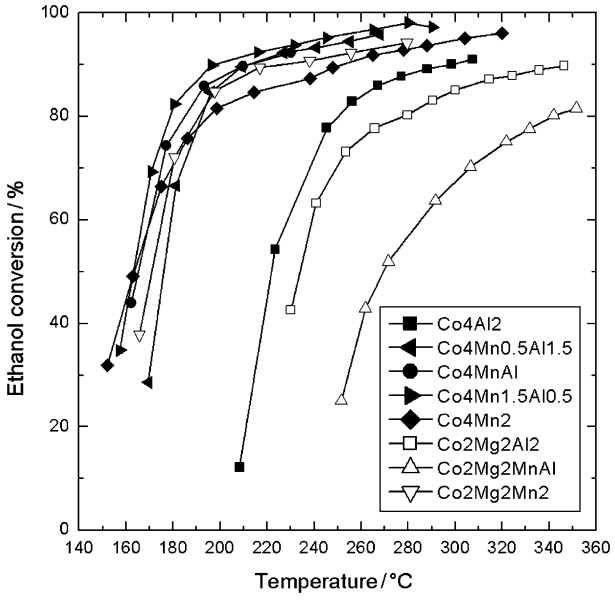

Fig. 11. Total oxidation of ethanol over catalysts prepared by calcination of formed LDH precursors at 500 °C. Conditions: ethanol concentration in air 1.0 g m^{-3}, total flow of 2.5 l h^{-1}, heating rate 3.5 °C min^{-1}, catalyst weight 0.75 g.

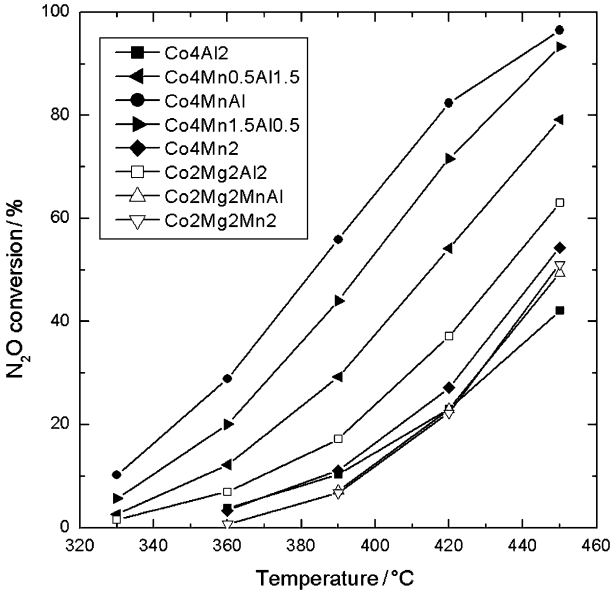

Fig. 12. Temperature dependence of N_2O conversion over catalysts prepared by calcination of formed LDH precursors at 500 °C. Conditions: 1000 ppm N_2O balanced by He, total flow of 100 ml min^{-1}, catalyst weight 0.1 g.

350–450 °C is necessary for achieving high catalytic activity in N_2O decomposition [21]. The existence of such optimum can be explained by using the concept of polaron hopping mechanism [32] in connection with oxidation–reduction mechanism of N_2O decomposition. It was found that on doping an inert matrix with transition metal cations from zero to the certain concentration (dependent on the matrix), the catalytic activity for some simple reactions including N_2O decomposition increases until each polaron (i.e. *d*-electron and its polarized environment) has at least one polaron nearest neighbor. The critical concentration at which the phenomenon proceeds is called 'the localized–nonlocalized point' (LNL point). After achieving LNL point the movement of polarons is relatively easy, the bulk electron will tend to fill in the empty orbital and the catalytic activity in N_2O decomposition decreases, probably due to a restriction of oxygen desorption from catalyst surface, which is the limiting step of the reaction [33].

4. Conclusions

The layered double hydroxides Co–M^{III} and Co–Mg–M^{III} (M^{III} = Mn and/or Al) were prepared and their thermal decomposition and formation of related mixed oxides were studied. The synthesis of LDH was not successful in system containing exclusively Co and Mn. The precursors obtained were decomposed at 200–300 °C to form nanocrystalline spinels, in Mg-containing systems spinels with low occupation of tetrahedral sites. The calcined samples were composed of spinels up to rather high temperatures (800–900 °C). At increasing temperature both crystallite size and content of XRD crystalline component increased. Raman spectroscopy and XRD

revealed segregation of Co-rich spinel in Co–Mn and Co–Mn–Al samples calcined at low temperatures. The presence of Mg in calcined samples inhibited the growth of spinel crystallites and stabilized larger mean (Co + Mn) valence. The calcined samples with high (Co + Mn) content were the most active in total oxidation of ethanol. Such simple relation was not observed in N_2O decomposition, where the highest activity exhibited the catalyst prepared by calcination of Co–Mn–Al LDH with Co:Mn:Al molar ratio of 4:1:1. The high activity of Co4MnAl catalyst can be explained by an optimum content of reducible components.

Acknowledgments

This work was supported by the Grant Agency of Czech Republic (Grant Projects Nos. 104/04/2116 and 106/05/0366) and by the Czech Ministry of Education, Youth and Sports (Research Projects Nos. MSM 6046137302 and 6198910016). The authors thank to Petr Vorm (Institute of Inorganic Chemistry, AS CR, Řež) for the synthesis of reference spinel oxides and Eva Večerníková (Institute of Inorganic Chemistry, AS CR, Řež) for performing thermal analyses.

References

[1] F. Cavani, F. Trifiro, A. Vaccari, Catal. Today 11 (1991) 173–301.
[2] A. Vaccari, Catal. Today 41 (1998) 53–71.
[3] T. Hibino, Y. Yamashita, K. Kosuge, A. Tsunashima, Clays Clay Miner. 43 (1995) 427–432.
[4] M.J. Hudson, S. Carlino, D.C. Apperley, J. Mater. Chem. 5 (1995) 323–329.
[5] M. Bellotto, B. Rebours, O. Clause, J. Lynch, D. Bazin, E. Elkaim, J. Phys. Chem. 100 (1996) 8535–8542.
[6] V. Rives, in: V. Rives (Ed.), Layered Double Hydroxides: Present and Future, Nova Science Publishers, New York, 2001, pp. 115–137.
[7] E. Kanezaki, Inorg. Chem. 37 (1998) 2588–2590.
[8] Ts. Stanimirova, I. Vergilov, G. Kirov, N. Petrova, J. Mater. Sci. 34 (1999) 4153–4161.
[9] A. De Roy, C. Forano, J.P. Besse, in: V. Rives (Ed.), Layered Double Hydroxides: Present and Future, Nova Science Publishers, New York, 2001, pp. 1–37.
[10] S. Kannan, C.S. Swamy, Catal. Today 53 (1999) 725–737.
[11] J. Pérez-Ramírez, F. Kapteijn, J.A. Moulijn, Catal. Lett. 60 (1999) 133–138.
[12] L. Chmielarz, P. Kustrowski, A. Rafalska-Lasocha, D. Majda, R. Dziembaj, Appl. Catal. B 35 (2002) 195–210.
[13] J.J. Spivey, Ind. Eng. Chem. Res. 26 (1987) 2165–2180.
[14] J. Pérez-Ramírez, G. Mul, F. Kapteijn, J.A. Moulijn, J. Mater. Chem. 11 (2001) 821–830.
[15] S. Kannan, C.S. Swamy, J. Mater. Sci. 32 (1997) 1623–1630.
[16] V. Rives, A. Dubey, S. Kannan, Phys. Chem. Chem. Phys. 3 (2001) 4826–4836.
[17] M.A. Pérez Bernal, R.J. Ruano Casero, V. Rives, Ceram. Silikáty 12 (2004) 145–154.
[18] J.M. Fernandez, C. Barriga, M.-A. Ulibarri, F.M. Labajos, V. Rives, J. Mater. Chem. 4 (1994) 1117–1121.
[19] T. Grygar, T. Rojka, P. Bezdička, E. Večerníková, F. Kovanda, J. Solid State Electrochem. 8 (2004) 252–259.
[20] F. Kovanda, T. Grygar, V. Dorničák, T. Rojka, P. Bezdička, K. Jirátová, Appl. Clay Sci. 28 (2005) 121–136.
[21] L. Obalová, K. Jirátová, F. Kovanda, K. Pacultová, Z. Lacný, Z. Mikulová, Appl. Catal. B 60 (2005) 289–297.
[22] F. Kovanda, T. Grygar, V. Dorničák, Solid State Sci. 5 (2003) 1019–1026.
[23] V. Rives, S. Kannan, J. Mater. Chem. 10 (2000) 489–495.
[24] A. Alejandre, F. Medina, P. Salagre, X. Correig, J.E. Sueiras, Chem. Mater. 11 (1999) 939–948.
[25] J. Zuo, C.Y. Xu, Y.P. Liu, Y.T. Qian, Nanostruct. Mater. 10 (1998) 1331–1335.
[26] B.A. Sexton, A.E. Hughes, T.W. Turney, J. Catal. 97 (1986) 390–406.
[27] Y. Lin, W. Chen, Mater. Chem. Phys. 85 (2004) 171–175.
[28] P. Arnoldy, J.A. Moulijn, J. Catal. 93 (1985) 38–54.
[29] M. Ferrandon, J. Carnö, S. Järas, E. Björnbom, Appl. Catal. A 180 (1999) 141–151.
[30] F. Kapteijn, L. Singoredjo, A. Andreini, J.A. Moulijn, Appl. Catal. B 3 (1994) 173–189.
[31] S. Ribet, D. Tichit, B. Coq, B. Ducourant, F. Morato, J. Solid State Chem. 142 (1999) 382–392.
[32] P. Pomonis, J.C. Vickerman, J. Catal. 55 (1978) 88–99.
[33] F. Kapteijn, J. Rodriguez-Mirasol, J.A. Moulijn, Appl. Catal. B 9 (1996) 25–64.